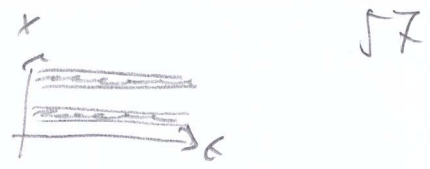


# 4.4 Beispiele von unendlichen Mustern



Wiederholung: - Turing: zeitlich konstantes Muster  
 - Hopf: homogene Oszillationen

Frage: gibt es das auch gleichzeitig?

↳ W. Just et al. PRL 64, 026219 (2000)

$$2 \text{ Variablen-Modell: } \frac{\partial u}{\partial t} = \alpha [j_0 - (u - a)] + D \left[ \frac{\partial^2 u}{\partial x^2} + \frac{\partial^2 u}{\partial y^2} \right]$$

$$\frac{\partial a}{\partial t} = \frac{u - a}{1 + (u - a)^2} - T a + \frac{\partial^2 a}{\partial x^2} + \frac{\partial^2 a}{\partial y^2}$$

$u$ : Spannung,  $a$ : Ladungsströmungsdichte,  $T$ : Tunnelrate

W. JUST, M. BOSE, S. BOSE, H. ENGEL, AND E. SCHÖLL

PHYSICAL REVIEW E 64 026219

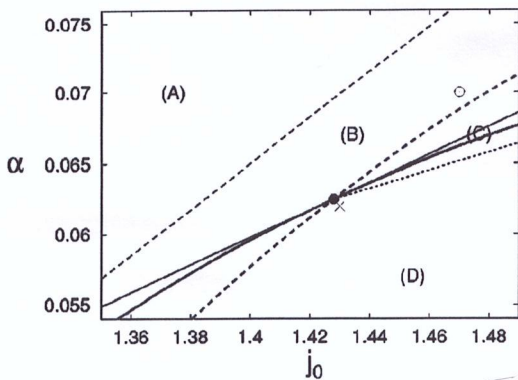


FIG. 3. Different stability regimes in the vicinity of the Turing-Hopf point (full circle) in the  $(j_0, \alpha)$  parameter plane. Gray: Turing (broken) and Hopf (full) bifurcation line (see Fig. 1). Existence of Hopf mode [full line, see Eq. (33)], stability of Hopf mode [dotted line, see Eq. (34)], and saddle-node bifurcation of Turing patterns [broken line, see Eq. (60)]. Region (A): trivial solution, region (B): coexistence between trivial solution and Turing pattern, region (C): Turing pattern, region (D): coexistence between Hopf mode and Turing pattern.  $\times$  and  $\circ$  mark the parameter settings used in Figs. 4 and 7, respectively.

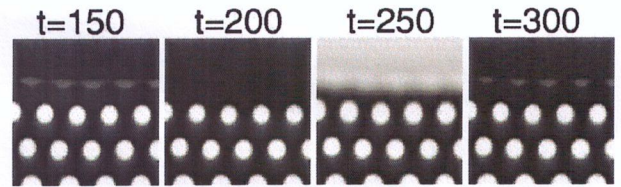
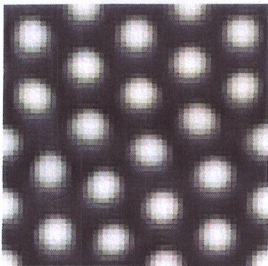


FIG. 5. Coexistence pattern between Turing and Hopf state at  $j_0 = 1.43$  and  $\alpha = 0.045$ . The density plots show the current density  $j(r, t)$  at four different times. The time labels refer to Fig. 6.

(a)



(b)

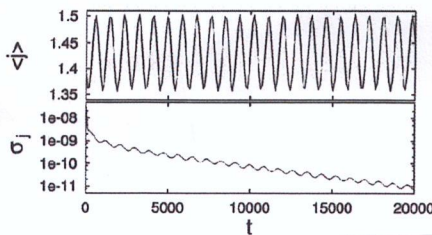


FIG. 4. (a) Density plot of stationary Turing pattern for the current density  $j(r, t) = u(r, t) - a(r, t)$ . (b) Relaxation of a Hopf mode. Time dependence of the spatial average  $\langle j \rangle$  of the current and the corresponding variance  $\sigma_j = \langle j^2 \rangle - \langle j \rangle^2$ . Parameter settings for both parts are the same ( $j_0 = 1.43$ ,  $\alpha = 0.062$ ,  $D = 5$ , and  $T = 0.05$ , see Fig. 3), but different initial conditions had been chosen.

PHYSICAL REVIEW E 64 026219

SPATIOTEMPORAL DYNAMICS NEAR A...

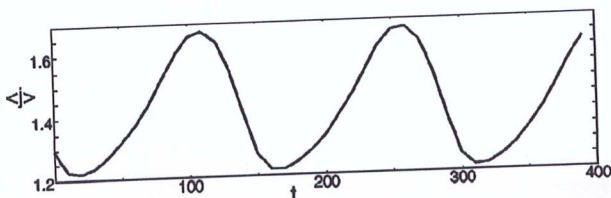


FIG. 6. Time dependence of the spatial average of the current

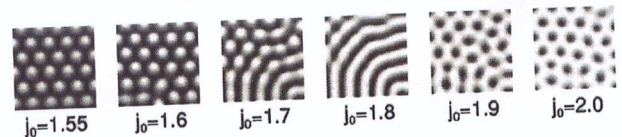
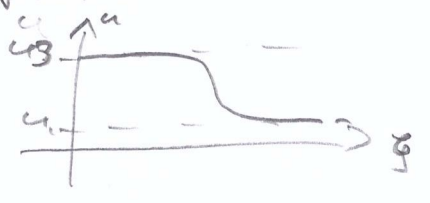


FIG. 8. Time independent patterns appearing for different values of the total current  $j_0$  at  $\alpha = 0.075$ ,  $T = 0.05$ , and  $D = 5$ : Transition from hot spots (left) to cold spots (right). Simulations have been performed on a system of size  $200 \times 200$  with Neumann boundary conditions.

Beweis zu Front-Lösung:

$$\frac{\partial u}{\partial t} = f(u) + D \frac{\partial^2 u}{\partial x^2} \xrightarrow{\xi = x - ct} Du'' + Cu' + f(u) = 0$$

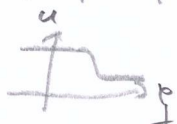


Bestimme C allgemein:

Idee: Multiplizieren mit \$u'\$ und integrieren:

$$D \int_{-\infty}^{\infty} d\xi \frac{d^2 u}{d\xi^2} \frac{du}{d\xi} + C \int_{-\infty}^{\infty} d\xi \left(\frac{du}{d\xi}\right)^2 + \int_{-\infty}^{\infty} d\xi f(u) \frac{du}{d\xi} = 0$$

$$= \frac{1}{2} D \left(\frac{du}{d\xi}\right)^2 \Big|_{-\infty}^{\infty} = 0 \qquad = \int_{u_1}^{u_3} du f(u) = A$$



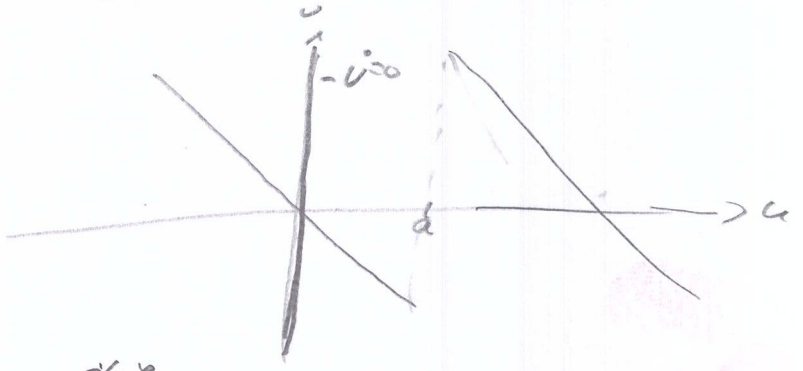
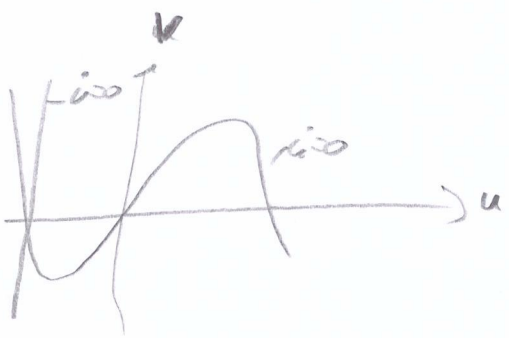
$$\Rightarrow C = \frac{\int_{u_1}^{u_3} du f(u)}{\int_{-\infty}^{\infty} d\xi \left(\frac{du}{d\xi}\right)^2}$$

$> 0$  für  $A > 0$ : Zündfront ungeschaltet ( $u_1$  metastabil)  
 $< 0$  für  $A = 0$ : Gleichgewichtswelle  
 $< 0$  für  $A < 0$ : Löschefront ( $u_3$  metastabil)

Approximation des Fitzhugh-Nagumo-Modell

$$\begin{cases} \epsilon \frac{\partial u}{\partial t} = u - \frac{u^3}{3} - v + \frac{\partial^2 u}{\partial x^2} \\ \frac{\partial v}{\partial t} = u + a \end{cases} \rightarrow \begin{cases} \frac{\partial u}{\partial t} = -u - H(u-a) + \frac{\partial^2 u}{\partial x^2} \\ \frac{\partial v}{\partial t} = \epsilon u \end{cases}$$

$H(u-a) = \begin{cases} 0 & u \leq a \\ 1 & u > a \end{cases}$



\$\Rightarrow\$ Störweite linear \$\Rightarrow\$ Lösung aus A1 & A2 zusammensetzen

(John Rinzel, Joseph B. Keller Biophys. Journal 13, 1313 (1973))

$\rho \propto Z$ :

$$\begin{aligned}\dot{\alpha} &= s(\eta - \eta\alpha + \alpha - q\alpha^2), \\ \dot{\eta} &= s^{-1}(-\eta - \eta\alpha + f\rho), \\ \dot{\rho} &= w(\alpha - \rho).\end{aligned}\tag{2.5}$$

The parameters  $s, w$  and  $q$  are determined from the rates of the reactions, see [29, 25].

Krug et al. introduced in [30] the modified Oregonator model, which describes the light sensitivity of the Belousov-Zhabotinsky reaction. For this purpose, the reaction scheme (2.3) was extended by a simple reaction, corresponding to the light-induced bromide flow



which leads to the modified three-component Oregonator model, given by

$$\begin{aligned}\epsilon\dot{x} &= x(1-x) + y(q-x), \\ \epsilon'\dot{y} &= \phi + fz - y(q+x), \\ \dot{z} &= x - z.\end{aligned}\tag{2.6}$$

The parameter  $\phi$  accounts for the light intensity. The following parameter values were suggested:  $q = 2 \times 10^{-3}$ ,  $f = 2.1$ ,  $\epsilon = 0.05$ ,  $\epsilon' = \epsilon/8$ . With this set of parameters, it was found that for  $\phi = 1.762 \times 10^{-3}$  the stable equilibrium in Eq. (2.6) undergoes a Hopf bifurcation, thus giving access to both excitable (monostable) and oscillatory reaction kinetics upon variation of the parameter  $\phi$  near the bifurcation value.

Often, one can exploit the smallness of the parameter  $\epsilon'$  and set the left-hand side of the second equation in Eq. (2.6) equal zero. In this case the model can be further reduced to the so-called two-component version of Oregonator, which reads

$$\begin{aligned}\dot{u} &= \frac{1}{\epsilon} \left[ u - u^2 - (fv + \phi) \frac{u - q}{u + q} \right], \\ \dot{v} &= u - v.\end{aligned}\tag{2.7}$$

We would like to mention that Eq. (2.7) is qualitatively similar to the FitzHugh-Nagumo equation [9, 10], which describes the propagation of the action potential in the squid axons.

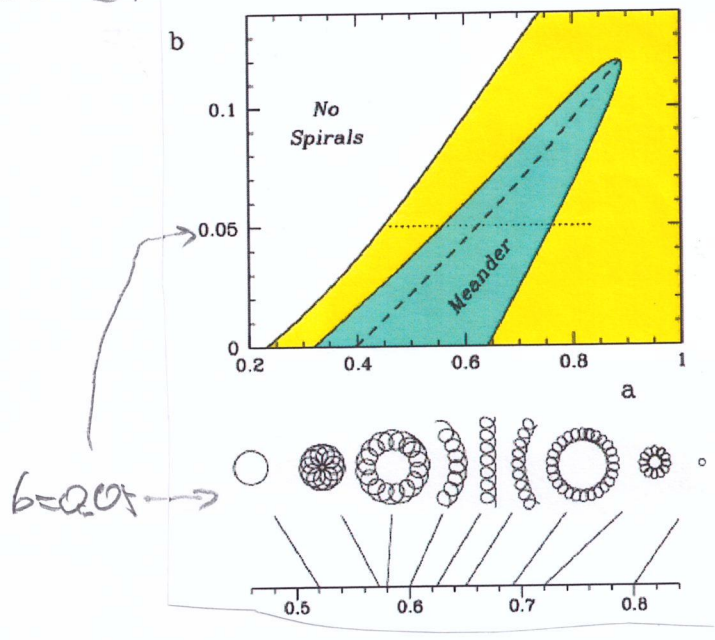
For spatially extended Belousov-Zhabotinsky reaction we must account for diffusion:

$$\begin{aligned}\partial_t u &= \frac{1}{\epsilon} \left[ u - u^2 - (fv + \phi) \frac{u - q}{u + q} \right] + D\Delta u, \\ \partial_t v &= u - v.\end{aligned}\tag{2.8}$$

Barkley-Kocbell:  $\frac{\partial u}{\partial t} = \frac{1}{\epsilon} u(1-u) \left( c - \frac{v+b}{\omega} \right) + \Delta u$

$\frac{\partial v}{\partial t} = u - v$

Dwight Barkley: *Physica D* 49, 67 (1991)  
 + Daele *IJBC* 8, 2529 (1997)



Oregan-Kocher Model: (2D)

$\frac{\partial u}{\partial t} = \frac{1}{\epsilon} \left[ u(1-u) - (f v + \phi) \frac{u-q}{u+q} \right] + D \Delta u$

$\frac{\partial v}{\partial t} = u - v$

Disselkreiffen Grigory Bardyuzov (2006)

V. Zykov et al.: *PRL* 92, 044301 (2004)

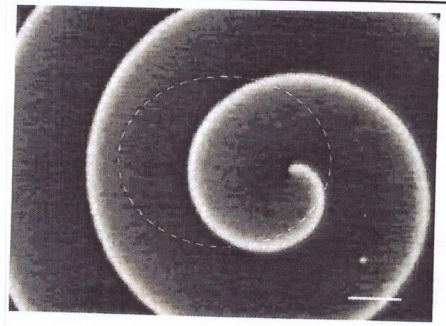


FIG. 1. Snapshot of a spiral wave rotating in a thin layer of the BZ reaction. The dashed line indicates the boundary of the wave.

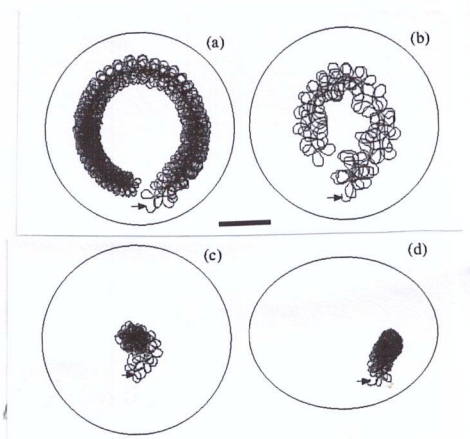


FIG. 2. Resonant drift of a spiral wave induced by a global feedback with  $k_{fb} = -1.5$ ,  $B_0 = 25$ , and  $I_0 = 70$ . (a)-(c) Circular domain of radius  $R = \lambda$ ; (d) elliptical domain with large axis  $a = 2\lambda = 4$  mm and small axis  $b = a/1.25$ . In (a) and (d), the time delay is  $\tau = 0$ , in (b)  $\tau/T_\infty = 0.32$ , and in (c)  $\tau/T_\infty = 0.5$ . Initial spiral tip locations are marked by arrows. Scale bar: 1 mm.